

# The influence of discrete surface charges on the force between charged surfaces

Malek O. Khan,<sup>a)</sup> Simon Petris, and Derek Y. C. Chan

*Department of Mathematics & Statistics, Particulate Fluids Processing Centre,  
The University of Melbourne, Parkville, Victoria 3010, Australia*

(Received 1 September 2004; accepted 14 December 2004; published online 10 March 2005)

The force between two parallel charged flat surfaces, with discrete surface charges, has been calculated with Monte Carlo simulations for different values of the electrostatic coupling. For low electrostatic coupling (small counterion valence, small surface charge, high dielectric constant, and high temperature) the total force is dominated by the entropic contribution and can be described by mean field theory, independent of the character of the surface charges. For moderate electrostatic coupling, counterion correlation effects lead to a smaller repulsion than predicted by mean field theory. This correlation effect is strengthened by discrete surface charges and the repulsive force is further reduced. For large electrostatic coupling the total force for smeared out surface charges is known to be attractive due to counterion correlations. If discrete surface charges are considered the attractive force is weakened and can even be turned into a repulsive force. This is due to the counterions being strongly correlated to the discrete surface charges forming effective, oppositely directed, dipoles on the two walls. © 2005 American Institute of Physics.  
[DOI: 10.1063/1.1856925]

## I. INTRODUCTION

The theoretical cornerstone of colloidal stability is the Derjaguin–Landau–Verwey–Overbeek (DLVO) theory,<sup>1,2</sup> in which attractive van der Waals forces are balanced by repulsive electrostatic interactions. In the DLVO theory, electrostatics are treated with the Poisson–Boltzmann (PB) mean field approximation. Although successful for a vast range of charged systems, it has been shown that the PB approximation is qualitatively incorrect when the electrostatic interactions are strong,<sup>3,4</sup> such as when multivalent counterions are present or when the dielectric constant of the solvent is small. Furthermore, the DLVO theory does not handle specific ion effects which can be important at high salt concentrations,<sup>5</sup> hydration forces which arise due to the specific structure of water,<sup>6</sup> or the discreteness of surface charges.<sup>7–12</sup>

In this paper we will describe the effect of discrete surface charges, either fixed in a lattice or mobile on the wall. Using Monte Carlo (MC) simulations the effective force between colloidal particles are calculated while varying a number of parameters, including the electrostatic coupling strength, the degree of charge discretization and the effect of multivalent ions. It turns out that for some sets of parameters the simulation results are qualitatively different from the mean field predictions.

A suitable model system which has drawn much interest is that of two parallel charged plates with only counterions, treated in the primitive model. The sole property of the solute is to screen electrostatic interactions by the dielectric constant  $\epsilon$  and the only interaction between charged particles

is of Coulomb type. The parallel plate geometry can be seen as a simple model for understanding colloidal stability but it also has a more direct experimental equivalent in lipid bilayers.<sup>13,14</sup> For the model system, the PB theory predicts that the electrostatic interaction between the plates is always repulsive. Monte Carlo simulations<sup>3</sup> and theories based on integral equations<sup>4</sup> have shown that when the counterions are divalent it is possible to observe an effective attraction between the plates. This attraction is attributed to counterion correlations which are not accounted for in the PB theory.

In both mean field theories and the early numerical work<sup>3,4</sup> the parallel surfaces or walls are assumed to have a smeared out uniform charge, quantified by a surface charge density  $\sigma$ . The validity of this approximation has been questioned when considering nanoscale systems where the macromolecules are of a size comparable to the average distance between them.<sup>15</sup> Even for the model case of infinite charged walls, simulations have shown how the discrete nature of the surface charge density will change the counterion distribution. Discrete surface charge will enhance the attraction of the counterions towards the wall and deplete the counterion distribution at the midplane between the walls.<sup>7–9</sup>

The effect of charge discretization on the effective interaction between the two walls have recently been approached theoretically. The result of charge discretization in mean field theories can be either to make the charged walls less repulsive<sup>12,10</sup> or more repulsive<sup>11</sup> depending on if all counterions reside between the walls or not. In this paper we will adopt the first approach and use Monte Carlo simulation to calculate exactly (within statistical limits) the effective interaction between two walls with discrete wall charges. The above mean field calculations are all performed for conditions at which the two plates repel each other. We will also

<sup>a)</sup>Author to whom correspondence should be addressed; Electronic mail: m.khan@ms.unimelb.edu.au

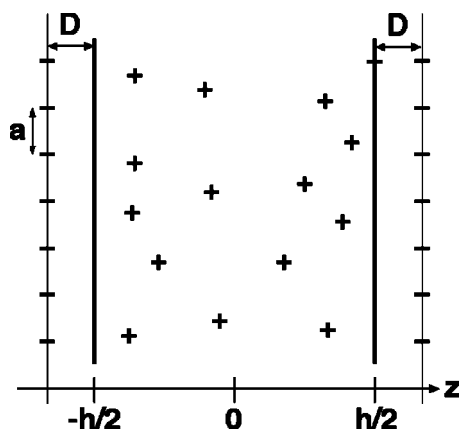


FIG. 1. In the model used, negative wall charges are located a distance  $D$  behind the walls. In the  $xy$  plane, the wall charges are distributed on a square lattice with lattice constant  $a$ . The walls are infinite in the  $xy$  plane and separated a distance  $h$  in the  $z$  direction.

investigate the effect of discrete charges when the electrostatic interactions are large, i.e., when a treatment including electrostatic correlation predicts an attraction between two walls with smeared out surface charge. Furthermore we will describe the effect of letting the wall ions move in directions lateral to the wall.

The remainder of this paper is organized as follows. Section II describes the model and the Monte Carlo method used to solve it. We will also introduce the different independent parameters of the model. In Sec. III, we present results showing where in this parameter space the effect of charge discretization is important. In Sec. IV, our results are summarized.

## II. THE MODEL AND NUMERICAL METHOD

### A. The model for two charged walls with counterions

The model charge surfaces are parallel, infinite in  $x$  and  $y$  directions, and located at  $z = \pm h/2$ , see Fig. 1. The walls have discrete negative charges located at  $z = \pm(D + h/2)$ . The neutralizing counterions are treated as point charges confined in  $-h/2 \leq z \leq h/2$ . The distance  $D$  is the distance of closest approach between the surface and counterions, and can be thought of as the size of the ions. No added salt is considered in this work. In the cases where the wall ions are positioned in a fixed square grid, the distance between the surface charges is  $a$ . The relation between the surface charge density  $\sigma$  and  $a$  is  $\sigma = Qe/a^2$ , where  $Q$  is the valence of the wall charges (without sign). The primitive model is used, where the solvent only enters by screening Coulomb interactions with the dielectric permittivity  $\epsilon_r \epsilon_0$ .  $\epsilon_0$  is the permittivity of vacuum and  $\epsilon_r$  is the relative dielectric constant of the solvent.

In this system there are four independent variables which are the following.<sup>8</sup>

(1) The coupling strength  $\Xi = q^2 l_B / \lambda_{GC} = 2\pi q^3 l_B^2 \sigma$ , where  $q$  is the counterion valence.  $l_B = e^2 / (4\pi\epsilon_r \epsilon_0 kT)$  is the Bjerrum length, the distance for which the interaction between two monovalent charges equals the thermal energy  $kT$  ( $l_B = 7.14 \text{ \AA}$  in water). The Gouy–Chapman length,  $\lambda_{GC} = e / (2\pi q l_B \sigma)$ , is the distance from the wall a counterion is

required to be moved in order for the bare Coulomb energy to change by  $kT$ . The coupling strengths covered are  $1 \leq \Xi \leq 100$  which ranges from low to very high coupling.

(2) The degree of charge discretization  $a/D$  (see Fig. 1), where the limit of  $a/D = 0$  corresponds to smeared out surface charges. We report results for  $2 \leq a/D \leq 8$ . The low limit results are equivalent to results for smeared out surface charges while the high limit is well above the threshold for which discretization effects are observed.

(3)  $q/Q$ , i.e., counterion valence divided by wall ion valence. Here we will look at effects of monovalent and divalent species,  $1/2 \leq q/Q \leq 2$ .

(4)  $h$ , the distance between the walls, which will vary as  $5 \leq h \leq 40 \text{ \AA}$ .

For fixed wall charges the opposite walls can be in phase or out of phase, which will affect the effective interaction between the plates. Instead of considering the out of phase system we will consider a model in which the surface charges can move within the  $x$  and  $y$  dimensions that make up the infinite walls.

### B. The Monte Carlo method

In order to simulate two parallel infinite charged walls with counterions in between, certain approximations regarding the boundary conditions in the  $xy$  plane have to be considered. Here we use a modified version of the approach of Valleau, Ivkov, and Torrie.<sup>16</sup> In our study, the wall charges and counterions inside the central Monte Carlo cell are treated as discrete charges while all electrostatic interactions outside the central cell are treated in a mean field approximation adding a tail correction to the interactions inside the central Monte Carlo cell.

The Hamiltonian of the system is

$$U = \sum_i^{N_{tot}-1} \sum_{j=i+1}^{N_{tot}} u^{(ii)}(r_{ij}) + \sum_i^{N_{tot}} u^{(ix)}(\vec{r}_i), \quad (1)$$

where  $N_{tot}$  is the total number of charged particles in the minimum image cell.  $u^{(ii)}(r_{ij})$  is the pair interaction between two charges in the central cell and  $u^{(ix)}(\vec{r}_i)$  is the tail correction for a charge in the central cell.

The direct interaction between two charged particles  $i$  and  $j$ , in the central Monte Carlo cell, is given by Coulombs law,

$$u^{(ii)}(r_{ij}) = \frac{z_i z_j e^2}{4\pi\epsilon_r \epsilon_0 r_{ij}}, \quad (2)$$

where  $z_i$  and  $z_j$  are the valences of the two particles and  $r_{ij}$  is the distance between the particles.

The tail correction for an ion  $i$  can be found from

$$u^{(ix)} = u^{(iw)} - u^{(iM)} + u^{(i\infty)} - u^{(if)}, \quad (3)$$

where  $u^{(iw)}$  is the interaction between an ion and an infinite wall with smeared out charges and  $u^{(iM)}$  is the interaction between an ion and a wall in the minimum image cell with smeared out charge.  $u^{(i\infty)} - u^{(if)}$  accounts for the interaction between an ion and the mean field solution outside the central cell. Here  $u^{(i\infty)}$  is the interaction between an ion and the mean field over the entire slit (infinite in  $x$  and  $y$ ) and  $u^{(if)}$  is

the interaction between an ion and the mean field in the minimum image cell. These subtractions are needed so as not to double count the counterion-counterion interactions in the central cell already accounted for when summing Eq. (2) over all particles in the central cell.

In practice, the mean field is only used as an initial approximation, since during the simulation the actual distribution in the central cell is used to update the tail correction in a self-consistent way.<sup>16</sup> Note that the first term  $u^{(iw)}$  is a constant, independent of the position of the ion. Thus  $u^{(iw)}$  does not have to be calculated when generating new configurations in the simulation.

When comparing with the expression for walls with smeared out charges,<sup>16</sup>

$$u^{(ix)} = u^{(iw)} + u^{(iz)} - u^{(if)}, \quad (4)$$

the only difference is the term  $u^{(iMI)}$  which we subtract not to double count the interaction with the part of the wall located within the minimum image cell. The expression for  $u^{(iMI)}$  is derived in the same manner as the other terms in Eq. (3).<sup>17</sup>

At the start of the Monte Carlo simulation the counterions are distributed randomly in the central cell. A trial configuration is generated by translating a single counterion a random distance between 0 and  $\delta_{tr}$ . The energy of the trial configuration is calculated according to Eq. (1) and rejected or accepted according to the standard Metropolis Monte Carlo scheme.<sup>18-20</sup>

After an equilibration of  $10^6 - 10^7$  attempted moves, averages are gathered for a simulation length of  $10^7 - 3 \times 10^8$  attempted moves. Depending on the parameters of the simulation,  $\delta_{tr}$  is between 2 and 15 Å. For the results reported here, simulations consisting of 144 ions per wall are used. This leads to the number of counterions varying from 144 to 576 depending on  $q/Q$ . When increasing the size of the system no noticeable changes were observed, indicating that no size effects are present. Also, in order to verify our program we have favorably compared our counterion profiles for the case of low coupling and low degree of charge discretization with the counterion profiles from simulations in which the walls have smeared out wall charges.

### C. Calculating the pressure

The main output from the simulations is the wall-wall interaction. Throughout this work we will be reporting on the pressure lateral to the walls. The pressure (or force per area unit) between the two walls can be calculated at any plane parallel to the walls. It is well known that the midplane is preferred for reasons of numerical stability.<sup>3</sup> At the midplane the pressure can be calculated as<sup>21</sup>

$$P = kT\rho + P^{es}, \quad (5)$$

where the first (entropic) term comes from the concentration  $\rho$  of counterions at the midplane and the second term  $P^{es}$  is the electrostatic force per unit area acting across the midplane. For the case with a smeared out surface charge Valleau *et al.*<sup>16</sup> showed how the electrostatic pressure can be calculated as  $P^{(ii)} - P^{(if)}$  where the same notation is used as in Eq. (3). Just as for the Hamiltonian the pressure is modified

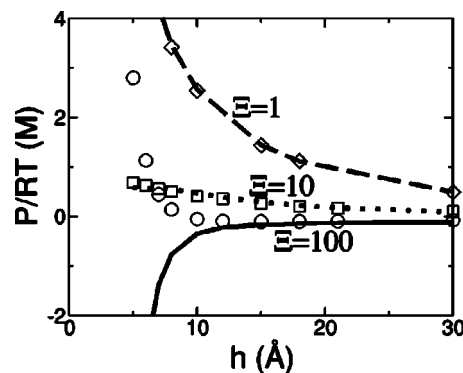


FIG. 2. The pressure as a function of the distance  $h$  between two charged walls ( $Q=1$ ) with monovalent counterions ( $q=1$ ). The lines are the results from MC simulations with a low degree of charge discretization ( $a/D=2$ ) while the symbols are results from corresponding simulations with a high degree of charge discretization ( $a/D=4$ ). The different coupling strengths are  $\Xi=1$  (dashed line and diamonds),  $\Xi=10$  (dotted line and squares) and  $\Xi=100$  (solid line and circles). The standard deviations are smaller than the symbol sizes.

since we need to subtract the interaction with a surface with smeared out charges in the central box,

$$P^{es} = P^{(ii)} - P^{(if)} - P^{(iMI)}. \quad (6)$$

In Eq. (6),  $P^{(ii)}$  is a double sum over all particles while the two last terms are single sums over all particles [compare with Eq. (1)].

It is interesting to study the separate components of the pressure as divided in Eq. (5). At the midplane the entropic part of the pressure is proportional to the ion concentration and always positive (repulsive). Mean field theories will only have this term always resulting in positive pressures.

For smeared out wall charges the electrostatic contribution  $P^{(ii)} - P^{(if)}$  is related to the deviation of the ionic distribution from its mean. Since a counterion in one-half of the slit will repel counterions in the other half,  $P^{(ii)} < P^{(if)}$  and the electrostatic pressure will always be negative (attractive).

When considering discrete wall charges, two different parts are added to the pressure. First,  $P^{(ii)}$  is now extended over the wall ions in the minimum image box and second,  $P^{(iMI)}$ , the interaction between counterions and the minimum image part of a wall with smeared out charges has to be subtracted [see Eq. (6)]. The resulting electrostatic pressure for discrete wall charges can be either repulsive or attractive depending on the electrostatic interactions.

In order to ensure convergence and good statistics we calculate the autocorrelation of  $P$  and adjust the length of the simulation so that at least a hundred independent observations of  $P$  are calculated. In most cases this number will be much higher.

### III. RESULTS AND DISCUSSION

We first consider the case where surface charges and counterions are monovalent  $q=Q=1$ . In Fig. 2 the pressure is shown as a function of the wall-wall separation for different coupling strengths  $\Xi$  and degrees of surface charge discretization  $a/D$ . At low coupling,  $\Xi=1$ , the discrete nature of the wall charges do not have any influence on the pressure. Increasing  $\Xi$  from 1 to 10 results in a decrease in pressure by

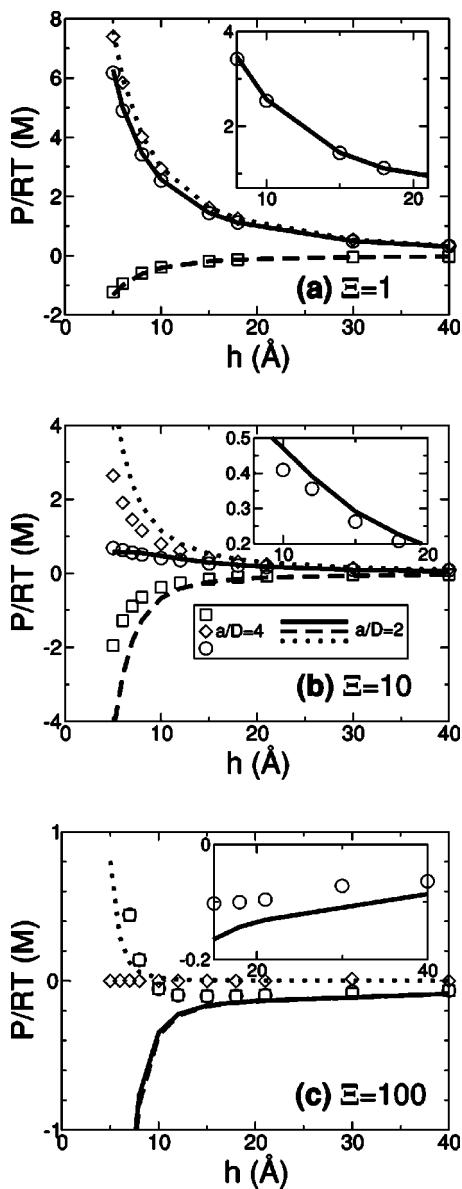


FIG. 3. The electrostatic correlation and entropic components of the total pressure for different coupling strengths (a)  $\Xi=1$ , (b)  $\Xi=10$ , and (c)  $\Xi=100$ . Results corresponding to a high degree of charge discretization ( $a/D=4$ ) are shown in symbols and those that correspond to a low degree of charge discretization ( $a/D=2$ ) are shown in lines. The electrostatic correlation components are given in squares and dashed lines, the entropic components are given in diamonds and dotted lines and the total pressures are given in circles and solid lines. The standard deviations are smaller than the symbol sizes (even for the insets).

a factor of 5 at  $h=21$  Å. This is in contrast to the prediction of mean field theory and demonstrates that counterion correlation is important in this regime.<sup>3,22</sup> On the scale of the figure, the discrete nature of the wall charges do not alter the pressure for  $\Xi=10$  either.

For smeared out surface charges and at high coupling, we expect counterion correlation effects to be large and that the total pressure should be attractive.<sup>3,22</sup> For  $\Xi=100$  this type of behavior can be observed for  $a/D=2$ , but when  $a/D=4$ , discrete surface charges lead to the total pressure being repulsive at small separation.

In Fig. 3 the electrostatic correlation and entropic components are shown together with the total pressure. For the

TABLE I. The entropic component  $P^{ent}$ , electrostatic component  $P^{es}$ , and the total pressure  $P$  for  $h=10$  Å,  $q=1$ , and  $Q=1$  at different degrees of charge discretization  $a/D$  and electrostatic coupling  $\Xi$ . Also shown is the standard deviation  $\sigma$  for the total pressure and the change in pressure when going from a low degree of charge discretization to a high degree of charge discretization,  $\Delta\% = 100\% (1 - [P(a/D=4)]/[P(a/D=2)])$ .

$a/D$	$\Xi$	$P^{ent}$ (mM)	$P^{es}$ (mM)	$P$ (mM)	$\sigma$ (mM)
2	10	1143	-673	470	3
4	10	790	-381	409	2
$\Delta\%$	10	31%	57%	13%	...
2	100	19	-360	-341	1
4	100	0	-52	-52	0.4
$\Delta\%$	100	100%	86%	85%	...

case of the coupling strength  $\Xi=1$  [Fig. 3(a)] the total pressure is due almost entirely to entropic effects and the electrostatic correlation component is not important. The two components, as well as the total pressure, are independent of the degree of charge discretization.

At a coupling strength of  $\Xi=10$  [Fig. 3(b)], the pressure is independent of  $a/D$  for large  $h$ , while for small  $h$  the total pressure is decreased slightly when increasing  $a/D$ , see the inset of Fig. 3(b). However, the relatively small change in total pressure with  $a/D$  is in fact made up of much larger relative changes in the entropic and electrostatic correlation components that happen to nearly cancel each other, see further Table I.

For  $\Xi=100$  [Fig. 3(c)] the two total pressure curves for  $a/D=4$  and  $a/D=2$  follow the electrostatic correlation contribution. For small  $h$  the electrostatic contribution to the pressure is attractive for a low degree of charge discretization and repulsive for a high degree of charge discretization, and consequently so are the total pressures. For large  $h$  the correlation induced attraction is reduced when increasing the degree of charge discretization, see the inset of Fig. 3(c). At  $h=21$  Å there is a 25% reduction in total (attractive) pressure when going from  $a/D=2$  to  $a/D=4$ .

Figure 4 gives an overview of the effect of discrete mobile and fixed surface charges at different coupling constants  $\Xi$  ( $a=8.4$  Å and  $h=10$  Å). For low electrostatic coupling, see inset of Fig. 4(a), the repulsive pressure is decreased with increasing degree of charge discretization. When going from  $a/D=2$  to  $a/D=8$  the pressure is decreased by around 15% for  $\Xi \leq 10$ . This confirms theoretical predictions by Lukatsky and Safran<sup>12</sup> for small  $\Xi$ .

At  $\Xi \approx 20$  the pressure is equal for the two cases of different degree of charge discretization. Just above  $\Xi=20$  the walls with a high degree of charge discretization have a larger repulsion than the walls with a low degree of charge discretization. For large  $\Xi$ , discrete surface charges results in a smaller wall-wall attraction than for walls with smeared out surface charges. The deviations for walls with discrete surface charges, compared to walls with smeared out wall charges, will increase when the relation  $a/h$  increases [see Fig. 3(c)]. Note that  $a$  appears in both the degree of charge discretization  $a/D$  and electrostatic coupling  $\Xi$ .

Figure 4(b) nicely illustrates that for the case with a low

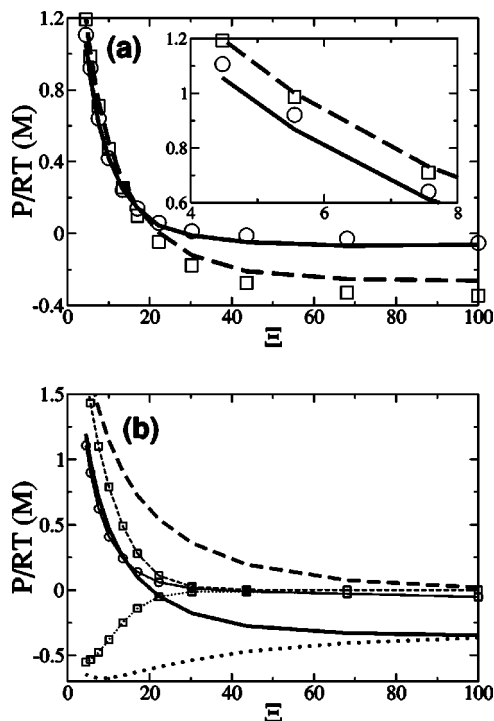


FIG. 4. The pressure between two charged walls as a function of the electrostatic coupling  $\Xi$  for  $q=1$ ,  $Q=1$ ,  $h=10$  Å, and  $a=8.4$  Å. (a) The lines are the results from MC simulations where the discrete wall charges are allowed to move while the symbols are results from the corresponding simulations with fixed discrete wall charges. The degrees of charge discretization are  $a/D=2$  (dashed line and squares) and  $a/D=8$  (solid line and circles). The inset shows corresponding results for small  $h$ . (b) The components of the pressure for the two cases with moving wall ions,  $a/D=2$  (lines without symbols) and  $a/D=8$  (lines with symbols). The solid lines shows the total pressure, the dotted lines the electrostatic correlation pressure, and the dashed lines the entropic pressure. The standard deviations are smaller than the symbol sizes.

degree of charge discretization (or smeared out wall charges), the decrease of the entropic repulsion is larger than the decrease of the electrostatic attraction when  $\Xi$  increases. The net attraction at high  $\Xi$  stems from the electrostatic counterion correlation attraction being changed less than the entropic repulsion.<sup>3</sup> Put another way, even if the electrostatic correlation attraction becomes smaller with increasing  $\Xi$ , it becomes relatively more important since the entropic repulsion decreases faster.

At small  $\Xi$  ( $<20$ ), the total pressure decreases only slightly with an increasing degree of charge discretization. This is deceptive, since in fact the entropic and correlation terms both change by a large percentage, but the sum remains almost unchanged. The same mechanism as that described above regarding counterion correlation for walls with smeared out wall charges can explain the decrease in pressure. Figure 5(a) shows that with increasing degree of charge discretization, counterions are more attracted towards the walls.<sup>7,8</sup> Obviously, with fewer counterions at the midplane the entropic contribution will be smaller. Even though the electrostatic contribution also decreases, it does not offset the decrease in the entropic contribution.

For large  $\Xi$  the entropic term approaches zero independent of the degree of charge discretization. For a small degree of charge discretization (or walls with smeared out sur-

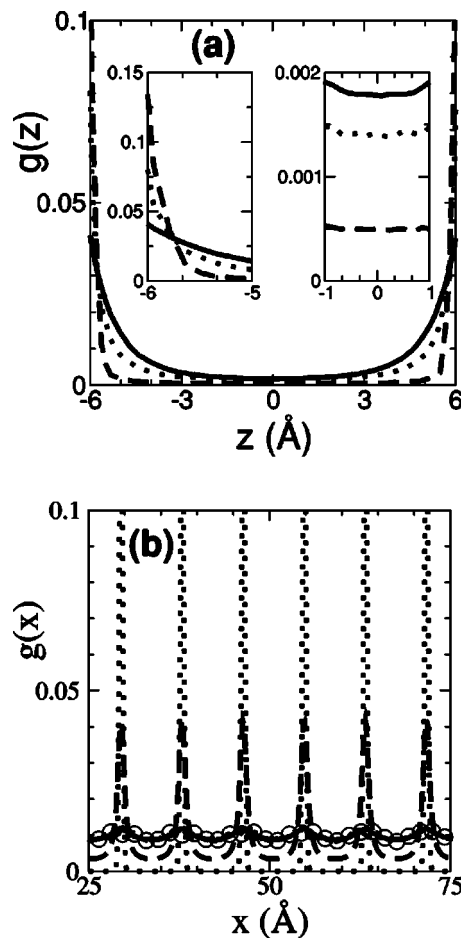


FIG. 5. Distribution functions for the counterions. (a) The distribution of counterions in the  $z$  direction, perpendicular to the walls, for  $a/D=2$  (solid line),  $a/D=4$  (dotted line), and  $a/D=8$  (dashed line).  $\Xi=10$  and  $h=12$  Å. The left inset provides details close to a wall and the right inset provides details around the midplane. (b) The distribution of counterions in the  $xy$  plane, parallel to the walls, for  $\Xi=1$  (solid line),  $\Xi=10$  (dashed line), and  $\Xi=100$  (dotted line).  $a/D=4$  and  $h=10$  Å. Also shown is the distribution for  $\Xi=100$ ,  $a/D=2$ , and  $h=10$  Å (circles). Only part of the wall in the minimal image box is shown.

face charges), counterion correlation effects will be important resulting in wall-wall attraction. For a large degree of charge discretization, electrostatic counterion correlation is much smaller (due to counterion-wall ion correlation, see below) resulting in a small attractive, or even repulsive, electrostatic pressure [see Fig. 3(c)].

The source of the qualitative difference of the electrostatic pressure component found for  $a/D=4$  and  $a/D=2$  in Fig. 3(c) can be found in the distribution of the counterions in the  $xy$  plane [Fig. 5(b)]. In the limit of low  $\Xi$  and small degree of charge discretization the distribution in the  $xy$  plane is almost uniform, approaching the case of smeared out surface charges. For  $a/D=4$  the counterions show a pronounced correlation around the discrete wall ions for high electrostatic coupling ( $\Xi=10$  and  $\Xi=100$ ). In the limit of very high  $\Xi$ , every counterion will effectively be localized around a wall ion, and the systems can be thought of as two walls with oppositely directed dipoles, which will have a repulsive interaction.

Note that for low degree of charge discretization, even

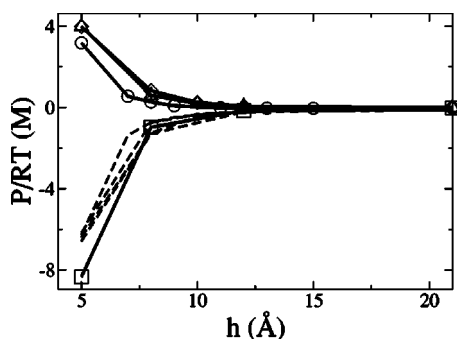


FIG. 6. The pressure between two charged walls as a function of the wall-wall distance for different values of  $q/Q$ . The dashed lines are the results from MC simulations where  $a/D=2$  while the solid lines with symbols are results from the corresponding simulations with  $a/D=8$ . The following values have been used,  $q=1:Q=1$  (circles), 2:1 (squares), 1:2 (diamonds), and 2:2 (triangles). The dashed lines are not individually labeled since they are similar. The simulations are performed for  $\Xi=100$ .

the high coupling case ( $\Xi=100$ ) does not give rise to strong deviation from the uniform distribution expected for smeared out wall charges which is why the counterions can still correlate to each other.

The effect of letting the wall ions move in a plane parallel to the walls, at a fixed distance  $D$  behind the wall, is shown in Fig. 4. The lattice constant  $a$  has no meaning but the quantity  $a/D$  will still be used as a measure of the degree of charge discretization ( $a$  can be thought of as constant describing the two-dimensional wall charge density). Figure 4 shows how letting the wall ions move, slightly increases the effect of discrete charges for small  $\Xi$ , while for large  $\Xi$  moving wall ions counteracts the effect of the discrete wall charges.

For small  $\Xi$  and a large degree of charge discretization the moving wall ions increase the attraction of the counterions towards the walls, in comparison to the case with fixed ions. According to the same reasoning as above this leads to both smaller repulsive entropic pressure and smaller attractive electrostatic correlation pressure, and since the entropic part changes more, the net result is a smaller repulsion. When  $\Xi$  is large it makes no difference if the wall ions are allowed to move, for large degree of charge discretization, since dipoles are formed in any case. For low degree of charge discretization, the moving wall ions again increase the attraction of the counterions towards the walls. Since the entropic pressure is negligible for large  $\Xi$ , the decrease of electrostatic attraction leads to a decrease in total attraction.

The last variable left to investigate is the valence of the ions. It is only for high  $\Xi$  that  $q/Q$  matters. For  $a/D=2$ , dashed lines in Fig. 6, the valence does not influence the result and all the lines are similar. For  $a/D=8$ , we have already seen that for  $q=1:Q=1$  the pressure becomes repulsive due to the formation of dipoles. The same behaviour should be true for  $q=2:Q=2$ , which Fig. 6 confirms. This is also evident for  $q=1:Q=2$ , where two monovalent counterions form an effective dipole with one divalent wall ion. For  $q=2:Q=1$ , the divalent counterions cannot form dipoles with the surface charges since the surface charges are fixed

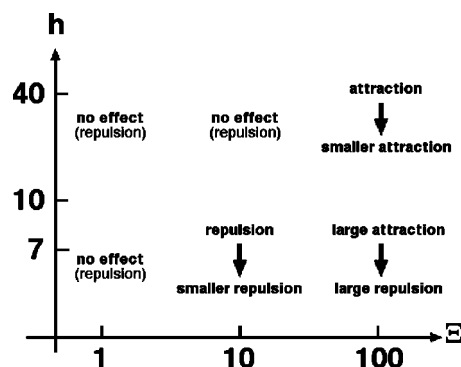


FIG. 7. A schematic overview of the effect of going from a low degree of charge discretization (or smeared out wall charges) to a high degree of charge discretization.

and thus the two walls attract each other for high  $\Xi$  and small  $h$ , just as walls with small degree of charge discretisation do.

#### IV. CONCLUSIONS

In this study we have shown that the effect of discrete wall charges can be important if the wall charges are located only a small distance into the wall and if the wall charges are far from each other. These effects are summarized in Fig. 7. Discrete wall charges modify the distribution of the counterions by attracting counterions towards the charged walls. For low  $\Xi$ , when entropy is dominating the system, increasing the degree of charge discretization mainly leads to a decrease in the repulsive entropic pressure component. This results in the total repulsive pressure decreasing. For large  $\Xi$ , when the electrostatic energy is large, the entropic component of the pressure disappears independent of the degree of charge discretization. For a small degree of charge discretization this leads to an attractive (electrostatic and total) pressure due to counterion correlation. For large  $h$  the effect of a large degree of charge discretization is to decrease this attractive pressure. For small wall-wall separations the attraction is turned into repulsion for a large degree of charge discretization since the counterions and wall charges form effective dipoles. This is true as long as the wall ion valence is a multiple of the counterion valence. Specifically the formation of dipoles is not possible for  $q=2:Q=1$ .

As pointed out by Moreira and Netz,<sup>8</sup> experimentally relevant systems can be affected by the inhomogeneous character of the surfaces. A system with  $\sigma=1/71 \text{ \AA}$  and only monovalent charges will have a lattice constant,  $a=8.4 \text{ \AA}$ , and  $\Xi=4.5$  for a water solution ( $\epsilon=78$ ) at room temperature. The repulsive pressure for such a system would be decreased due to discrete surface charges if  $h$  is smaller than 10–15  $\text{\AA}$  and  $D$  is around 2  $\text{\AA}$ .

In our simulations, a change from attraction to repulsion is found for  $\Xi>20$  and  $a/D>4$ . For a system with  $\sigma=1/128 \text{ \AA}^{-2}$  and divalent counterions as well as surface charges, the lattice constant is  $a=16 \text{ \AA}$ , and  $\Xi=20$  for a water solution at room temperature. For a minimal distance between wall ions and counterions of  $D\approx 4 \text{ \AA}$  the ratio

$a/D=4$  is obtained, which is at the start of the range for which discrete surface charges will lead to qualitative deviations from the case with smeared out surface charges.

## ACKNOWLEDGMENTS

This work was supported by the Australian Research Council, the Particulate Fluids Processing Centre at The University of Melbourne, the Victorian Partnership for Advanced Computing, and the Wenner–Gren Foundations.

<sup>1</sup>J. Israelachvili, *Intermolecular and Surface Forces*, 2nd ed. (Academic, London, 1991).

<sup>2</sup>D. F. Evans and H. Wennerström, *The Colloidal Domain: Where Physics, Chemistry, Technology and Biology Meet* (VCH, New York, 1994).

<sup>3</sup>L. Gulbrand, B. Jönsson, H. Wennerström, and P. Linse, *J. Chem. Phys.* **80**, 2221 (1984).

<sup>4</sup>R. Kjellander and S. Marčelja, *J. Chem. Phys.* **82**, 2122 (1985).

<sup>5</sup>M. Boström, D. R. M. Williams, and B. W. Ninham, *Phys. Rev. Lett.* **87**, 168103 (2001).

<sup>6</sup>J. N. Israelachvili and H. Wennerström, *Nature (London)* **379**, 219 (1996).

<sup>7</sup>T. Åkesson and B. Jönsson, *J. Phys. Chem.* **89**, 2401 (1985).

<sup>8</sup>A. G. Moreira and R. R. Netz, *Europhys. Lett.* **57**, 911 (2002).

<sup>9</sup>D. B. Lukatsky, S. A. Safran, A. W. C. Lau, and P. Pincus, *Europhys. Lett.* **58**, 785 (2002).

<sup>10</sup>L. Foret, R. Kühn, and A. Würger, *Phys. Rev. Lett.* **89**, 156102 (2002).

<sup>11</sup>T. O. White and J. P. Hansen, *J. Phys.: Condens. Matter* **14**, 7649 (2001).

<sup>12</sup>D. B. Lukatsky and S. A. Safran, *Europhys. Lett.* **60**, 629 (2002).

<sup>13</sup>A. Khan, K. Fontell, and B. Lindman, *J. Colloid Interface Sci.* **101**, 193 (1984).

<sup>14</sup>A. Khan, K. Fontell, and B. Lindman, *Colloids Surf.* **11**, 401 (1984).

<sup>15</sup>E. Allahyarov, H. Löwen, A. A. Louis, and J. P. Hansen, *Europhys. Lett.* **57**, 731 (2002).

<sup>16</sup>J. P. Valleau, R. Ivkov, and G. M. Torrie, *J. Chem. Phys.* **95**, 520 (1991).

<sup>17</sup>B. Jönsson, H. Wennerström, and B. Halle, *J. Phys. Chem.* **84**, 2179 (1980).

<sup>18</sup>N. A. Metropolis, A. W. Rosenbluth, M. N. Rosenbluth, A. Teller, and E. Teller, *J. Chem. Phys.* **21**, 1087 (1953).

<sup>19</sup>M. P. Allen and D. J. Tildesley, *Computer Simulation of Liquids* (Oxford University Press, Oxford, 1989).

<sup>20</sup>D. Frenkel and B. Smit, *Understanding Molecular Simulation* (Academic, San Diego, 1996).

<sup>21</sup>H. Wennerström, B. Jönsson, and P. Linse, *J. Chem. Phys.* **76**, 4665 (1982).

<sup>22</sup>A. G. Moreira and R. R. Netz, *Phys. Rev. Lett.* **87**, 078301 (2001).